Charge carrier effective mass and concentration derived from combination of Seebeck coefficient and ^{125}Te NMR measurements in complex tellurides

E. M. Levin

Phys. Rev. B **93**, 245202 — Published 27 June 2016

DOI: 10.1103/PhysRevB.93.245202

06-03-2016

Charge carrier effective mass and concentration derived from combination of Seebeck coefficient and ^{125}Te NMR measurements in complex tellurides

E. M. Levin

Division of Materials Sciences and Engineering, U.S. Department of Energy Ames Laboratory, Ames, Iowa 50011, USA
Department of Physics and Astronomy, Iowa State University, Ames Iowa 50011, USA

Submitted to *Physical Review B*

Abstract

Thermoelectric materials utilize the Seebeck effect to convert thermal to electrical energy. The Seebeck coefficient (thermopower), S, depends on the free (mobile) carrier concentration, n, and effective mass, m^*, as $S \sim m^*/n^{2/3}$. The carrier concentration in tellurides can be derived from ^{125}Te NMR spin-lattice relaxation measurements. NMR spin-lattice relaxation rate, $1/T_1$, depends on both n and m^* as $1/T_1 \sim (m^*)^{3/2} n$ (within classical Maxwell-Boltzmann statistics) or as $1/T_1 \sim (m^*)^2 n^{2/3}$ (within quantum Fermi-Dirac statistics), which challenges the correct determination of the carrier concentration in some materials by NMR. Here it is shown that the combination of the Seebeck coefficient and ^{125}Te NMR spin-lattice relaxation measurements in complex tellurides provides a unique opportunity to derive the carrier effective mass and then to calculate the carrier concentration. This approach was used to study $Ag_xSb_xGe_{50-2x}Te_{50}$, well-known GeTe-based high-efficiency TAGS thermoelectric materials, where the replacement of Ge by [Ag+Sb] results in significant enhancement of the Seebeck coefficient. Values of both m^* and n derived using this combination show that the enhancement of thermopower can be attributed primarily to an increase of the carrier effective mass and partially to a decrease of the carrier concentration when the [Ag+Sb] content increases.

PACS: 72.20.Pa; 76.60.-k; 76.60.Es
Keywords: $Ag_xSb_xGe_{50-2x}Te_{50}$ (TAGS); Seebeck coefficient; ^{125}Te NMR spin-lattice relaxation time; charge carrier effective mass and concentration.

The Seebeck effect demonstrates that temperature difference and heat flow across electrically conductive materials result in the appearance of an electric field. This is a very interesting fundamental phenomenon, connecting thermodynamics and electricity and enabling direct heat to electrical energy conversion by utilizing thermoelectric materials with a large Seebeck coefficient (thermopower), S [1-3]. Thermoelectric materials have been studied for a long time, but deep understanding of heat to electrical energy conversion in complex materials, i.e. the Seebeck effect itself, still is lacking.

The Seebeck coefficient of semiconductors generally decreases when the concentration of free (mobile) charge carriers (electrons or holes) increases, which is well established experimentally for thermoelectric tellurides and can be described by the Mott-Boltzmann formalism with energy independent carrier scattering. The Seebeck coefficient predicted by the theory for metals and degenerate semiconductors with a parabolic band and energy-independent charge carrier scattering depends on the carrier concentration of electrons or holes, n, and the effective mass, m^* [1] as

$$S = \frac{8\pi^2 k_B^2 T}{3eh^2} m^* \left(\frac{\pi}{3n}\right)^{2/3} \qquad (1)$$

In some materials the influence of m^* on the Seebeck coefficient can be significant and its determination is important for better understanding of thermoelectric materials.

^{125}Te nuclear magnetic resonance (NMR) [4-9] can be used to study complex tellurides and derive the carrier concentration from spin-lattice relaxation time, T_1. In a theoretical model by Selbach *et al*. [10], the coefficient of proportionality between T_1 and n, "Bloembergen constant", C_B, depends on m^*. Hence, if the effective mass in a series of materials is not constant, it can affect C_B, and, therefore, the carrier concentration deriving from ^{125}Te NMR T_1 measurements should be different compared to that obtained if m^* is constant.

Here it is shown that the combination of the Seebeck coefficient and ^{125}Te NMR spin-lattice relaxation measurements provides a unique opportunity to derive the carrier effective mass, then to

calculate the carrier concentration, and to elucidate their influence on the Seebeck coefficient. As a model system, $Ag_xSb_xGe_{50-2x}Te_{50}$ series, well-known GeTe-based high-efficiency tellurium-antimony-germanium-silver thermoelectric materials (TAGS series) [11-13], was used. The replacement of Ge by [Ag+Sb] results in the enhancement of the Seebeck coefficient while the carrier concentration also increases [12,13], which does not fit Eq 1. Typically TAGS materials are shown as $(GeTe)_m(AgSbTe_2)_{100-m}$ (TAGS-*m*) [11-13], which is inaccurate as the $AgSbTe_2$ compound is not used in synthesis and does not replace Ge; it is more convenient to use the equation $Ag_xSb_xGe_{50-2x}Te$, which reflects the replacement of Ge in the GeTe matrix by [Ag+Sb] atoms. However, in some cases it is convenient to show the composition of these alloys as TAGS-*m*, where *m* can change from 100 to 85, i.e. the [Ag+Sb] content changes from 0 to ~13 atomic % (at.%). These materials were developed by NASA in the 1970s and used for various applications [1-3,11], while their high efficiency was never explained.

$Ag_xSb_xGe_{50-2x}Te_{50}$ materials with different [Ag+Sb] content (Table 1) were synthesized by a direct reaction of the constituent elements in 10 mm diameter fused silica ampoules in argon back-filled up to ~17 kPa pressure atmosphere. For synthesis we used Ge (Materion G-1038, 99.999% purity), and Te (Alfa Aesar, 99.9999% purity, product #12607, lot 004). Ampoules with the constituent elements were heated up to 1323 K to melt the constituents, and after ~4 hours the melt was cooled down with the furnace at the rate of 100 K/hour. Each ingot had a mass of 20 g, diameter of 10 mm, length of ~40 mm. Analysis of each material was performed by X-ray diffraction, scanning electron microscopy, and energy dispersive spectroscopy, and showed that all materials are nearly single phase; only ~1 at.% Ge is present in the samples matrix due to naturally occurring process of Ge rejection from the melt [8,14]. ^{125}Te NMR experiments were performed at 126 MHz using a Bruker 400WB spectrometer with TOPSPIN software in a magnetic field of 9.4 T without sample spinning

(static regime). Powder samples were prepared from ingots and placed in 4-mm diameter insert. ^{125}Te NMR spin-lattice relaxation measurements were used to obtain the spin-lattice relaxation time, T_1, using GeTe as a reference material [5,8]; the uncertainty of T_1 measurements is less than ±0.2 ms [5]. More experimental details including pulse sequence for ^{125}Te NMR can be found in Refs. 5,8,9,14. Samples for the Seebeck coefficient measurements were prepared by cutting the ingot with a diamond saw [9]. The Seebeck coefficient was measured by a LSR-3 measuring system (Linseis Inc.) in a helium atmosphere relative to the Pt legs of a Pt-(Pt+Rh) thermocouple and then the absolute Seebeck coefficient was calculated; the uncertainty of measurements is about ±3% [9].

Figure 1(a) demonstrates ^{125}Te NMR spin-lattice relaxation via dependencies of normalized integrals vs. saturation recovery time at 300 K for the end compositions, GeTe and $Ag_{6.5}Sb_{6.5}Ge_{37}Te_{50}$ (TAGS-85). Relaxation curves for the rest of the materials studied here are between those for GeTe and TAGS-85 with the longest, 5.3 ms, and shortest, 3.1 ms, spin-lattice relaxation time, i.e. T_1 decreases with [Ag+Sb] content (see the values of T_1 for all materials studied in Table 1). ^{125}Te NMR spectra for these two materials are shown on inset in Fig. 1(a), demonstrating that signals can be easily detected; spectra for the rest of materials also are located between those for GeTe and TAGS-85. Relaxation curves shown on Fig. 1(a) as well as for the rest of materials can be fit by one component [5,14], i.e., GeTe and TAGS-85 and other materials studied here are electronically homogeneous [4,5,14].

Spin-lattice relaxation in electrically conductive materials is primarily produced by the hyperfine interaction between a nuclei and free (mobile) charge carriers (electrons or holes) and depends on the carrier concentration [10,15]. In thermoelectric tellurides, T_1 strongly depends on the carrier concentration: the higher carrier concentration, the shorter is T_1 [4,5].

The values of the Seebeck coefficient at 300 K of materials studied here are shown in Table 1; the inset in Fig. 1(b) shows this data as the S_{TAGS} / S_{GeTe} ratio at 300 K, i.e. they are normalized on the value of the Seebeck coefficient of GeTe. Our data agrees well with that reported for GeTe [16,17], TAGS-80, and TAGS-90 [12,13]. The Seebeck coefficient of our samples increases with [Ag+Sb] content from about +34 μV K^{-1} in GeTe to +83 μV K^{-1} in TAGS-85. Such an increase can, in principle, be explained, according to Eq. 1, by a reduction in the carrier concentration. However, the carrier concentration in TAGS-85 derived from the Hall effect is 12.1×10^{21} cm^{-3} [12] or 15.1×10^{21} cm^{-3} [13], which is higher than that in GeTe, $(8\pm1)\times10^{20}$ cm^{-3} [8,16,17]. Similarly, T_1 in TAGS materials is shorter than that of GeTe (Table 1), which, in principle, can be attributed to a higher charge carrier concentration. These discrepancies show that the carrier effective mass may have effect on the enhancement of the Seebeck coefficient in TAGS materials. It can be noted here that replacement of Ge in GeTe only by Ag in $Ag_xGe_{50-x}Te$ or by Sb in $Sb_xGe_{50-x}Te$ demonstrates quite different effects: Ag decreases whereas Sb increases the Seebeck coefficient via increasing or decreasing the carrier concentration, respectively [18]. Hence, the effect from separate replacement of Ge in GeTe by Ag or Sb is different compared to that when Ge is replaced by both Ag and Sb.

The relation between the spin-lattice relaxation rate $1/T_1$, carrier effective mass and concentration can be shown as $1/T_1 \sim (m^*)^{3/2} n$ based on classical Maxwell-Boltzmann statistics (used for semiconductors) or as $1/T_1 \sim (m^*)^2 n^{2/3}$ based on quantum Fermi-Dirac statistics (used for metals or highly degenerate semiconductors) [10,15]. If the carrier effective mass in GeTe-based materials does not change significantly, the carrier concentration can be estimated using GeTe with a carrier concentration of 8×10^{20} cm^{-3} (obtained from the Hall effect) and $T_1 = 5.3\pm0.2$ ms [5,8] as a reference. With Maxwell-Boltzmann statistics, at a given temperature (300 K), we can use the ratio

$$1/T_1 \sim n \qquad (2)$$

Hence, the carrier concentration in TAGS materials can be calculated as $n = n_r(T_{1,r})/(T_1)$, where n_r and $T_{1,r}$ are the carrier concentration and spin-lattice relaxation time of the GeTe reference.

However, if the carrier effective mass in GeTe-based materials changes with composition, it will affect the coefficient of proportionality between T_1 and n, which with Maxwell-Boltzmann statistics can be shown as

$$n \sim \frac{1}{(m^*)^{3/2} T_1} \tag{3}$$

Eq. 1 can be shown in a simpler form as

$$S \sim \frac{m^*}{n^{2/3}} \tag{4}$$

A combination of Eq. 3 and Eq. 4 shows that the Seebeck coefficient is proportional to the carrier effective mass and spin-lattice relaxation time as

$$S \sim (m^*)^2 T_1^{2/3} \tag{5}$$

Based on Eq. 5, at a given temperature (300 K), the ratio between the Seebeck coefficients of TAGS materials, S_{TAGS}, and GeTe reference material, S_{GeTe}, can be shown as

$$\frac{S_{TAGS}}{S_{GeTe}} = \left(\frac{m^*_{TAGS}}{m^*_{GeTe}}\right)^2 \left(\frac{T_{1,TAGS}}{T_{1,GeTe}}\right)^{2/3} \tag{6}$$

The combination of spin-lattice relaxation times, $T_{1,TAGS}$ and $T_{1,GeTe}$, and the Seebeck coefficients, S_{TAGS} and S_{GeTe}, allow us to calculate the carrier effective mass, m^*_{TAGS}, as

$$m^*_{TAGS} = m^*_{GeTe} \left(\frac{S_{TAGS}/S_{GeTe}}{(T_{1,TAGS}/T_{1,GeTe})^{2/3}}\right)^{1/2} \tag{7}$$

Eq. 7 allows us to calculate the m^*_{TAGS}/m^*_{GeTe} ratio vs. the [Ag+Sb] content in $Ag_xSb_xGe_{50-2x}Te_{50}$ materials using experimental data for the Seebeck coefficient and ^{125}Te NMR spin-lattice relaxation time from Table 1. Figure 1(b) demonstrates that the m^*_{TAGS}/m^*_{GeTe} ratio near linearly increases with [Ag+Sb] content and shows that the replacement of Ge in GeTe by ~13 at.% [Ag+Sb] increases the carrier effective mass by ~1.8 times that of GeTe (see also Table 1). Note that the effective mass of holes in GeTe is $m^* = 1.15\ m_0$, where m_0 is the mass of a free electron [19]; hence, m^* calculated for $Ag_{6.5}Sb_{6.5}Ge_{37}Te_{50}$ (TAGS-85) is larger than m_0 by 2.12 times (Table 1). The S_{TAGS}/S_{GeTe} ratio also increases near linearly with [Ag+Sb] content [see the inset in Fig. 1(b)], demonstrating the correlation between S and m^* in $Ag_xSb_xGe_{50-2x}Te_{50}$ materials.

Interestingly, the replacement of Ge in TAGS-85 by ~1 at.% the rare-earth Dy enhances the Seebeck coefficient up to +93 μV/K [9], while the spin-lattice relaxation time is similar to that of TAGS-85. Calculations performed by Eq. 7 show that $m^*_{TAGS-85+1\,at\%Dy}/m^*_{GeTe} = 1.98$ or $m^*_{TAGS-85+1\,at\%Dy}/m_0 = 2.28$. This demonstrates that carrier effective mass in TAGS materials can be increased by adding even a small amount of a rare-earth element with a large atomic size and localized magnetic moment.

The ratio between the carrier concentrations in TAGS, n_{TAGS}, and GeTe, n_{GeTe}, can be shown as

$$\frac{n_{TAGS}}{n_{GeTe}} = \left(\frac{m^*_{GeTe}}{m^*_{TAGS}}\right)^{3/2}\left(\frac{T_{1,GeTe}}{T_{1,TAGS}}\right) \tag{8}$$

Hence, the carrier concentration in TAGS materials relative to that in GeTe can be calculated as

$$n_{TAGS} = n_{GeTe}\left(\frac{m^*_{GeTe}}{m^*_{TAGS}}\right)^{3/2}\left(\frac{T_{1,GeTe}}{T_{1,TAGS}}\right) \tag{9}$$

Figure 2 demonstrates the difference in the calculated carrier concentration when two relations, (i) $1/T_1 \sim n$ (if m^* is constant) or (ii) $1/T_1 \sim (m^*)^{3/2} n$ (if m^* is not constant) based on classical Maxwell-Boltzmann statistics, are used. If the carrier effective mass does not change with [Ag+Sb] content, Eq. 2 should be used, and the carrier concentration increases with [Ag+Sb] content, which, in principle, agrees with the Hall effect data [12,13], but it is difficult to explain because a reduction in Ge may result in the reduction of Ge vacancies, which generate free holes in GeTe-based materials.

Alternatively, if the carrier effective mass increases with the [Ag+Sb] content, Eq. 9 should be used, and the carrier concentration decreases with [Ag+Sb] content. The latter agrees well with the expected reduction in both the concentration of Ge vacancies and free holes generated by these vacancies. A discrepancy with the Hall effect data reported in Refs. 12,13 can be explained by the presence of different scattering mechamnisms,[13] or by the affect from possible small amount of a second *n*-type phase like Ag_2Te. Shorter ^{125}Te NMR T_1 can be attributed to the effect from [Ag+Sb] pairs, which results in a larger density of electron states at the Fermi level.

If quantum Fermi-Dirac statistics is used, the effective mass and carrier concentration in TAGS materials can be calculated using modified equations (not shown here) because $1/T_1 \sim (m^*)^2 n^{2/3}$. The values of the carrier concentrations for TAGS materials in this case are slightly higher than that obtained by Maxwell-Boltzmann statistics. For example, the carrier concentration in TAGS-85 with T_1 = 3.1 ms calculated with Fermi-Dirac statistics is 6.8×10^{20} cm^{-3} (shown by blue diamond on Fig. 2), whereas that calculated with Maxwell-Boltzmann statistics is 5.5×10^{20} cm^{-3}. However, the trends for both statistics are similar: the carrier concentration slightly decreases, whereas the effective mass significantly increases with [Ag+Sb].

The enhancement of the Seebeck coefficient for $Ag_xSb_xGe_{50-2x}Te_{50}$ materials due to an increase in the carrier effective mass and a decrease in the carrier concentration can separately be estimated via

Eq. 7 and Eq. 9. Figure 3(a) shows the enhancement via the S_{TAGS} / S_{GeTe} ratio; all calculations are performed using Maxwell-Boltzmann statistics. The effect from the carrier effective mass is much larger compared to that from the carrier concentration, but the sum of both contributions is close to the experimentally observed value. The increase of the carrier effective mass in $Ag_xSb_xGe_{50-2x}Te_{50}$ in conjunction with [Ag+Sb] content agrees with that predicted for TAGS-85 by theoretical calculations [20], but our value is smaller.

Note that replacement of Ge in GeTe by only Sb in $Sb_xGe_{50-x}Te_{50}$ also enhances the Seebeck coefficient [18], but this effect is found to be mostly due to a significant decrease of the carrier concentration, which is usual effect. In contrast, replacement of GeTe by both [Ag+Sb] in $Ag_xSb_xGe_{50-2x}Te_{50}$ shown here enhances the Seecbeck coefficient whereas the carrier concentration does not decrease significantly, which is unusual effect. Replacement of Ge in GeTe by only Ag in $Ag_xGe_{50-x}Te_{50}$ decreases the Seebeck coefficient due to a higher carrier concentration [18], which is also usual effect. A comparison of the Seebeck coefficients and ^{125}Te NMR data for $Ag_xGe_{50-x}Te_{50}$, $Sb_xGe_{50-x}Te_{50}$, and $Ag_xSb_xGe_{50-2x}Te_{50}$ shows the existence of the [Ag+Sb] atomic pairs formed in TAGS materials [18]. Larger effective mass in TAGS materials can be explained by the interaction of the free (mobile) charge carriers with these pairs.

Figure 3(b) also shows the separate effects from the carrier effective mass and concentration as well as their simultaneous effect on the S_{TAGS} / S_{GeTe} ratio. It is interesting that both contributions can enhance heat to electrical energy conversion, and the simultaneous effect can explain the high efficiency of TAGS materials. Figures 3(a)(b) demonstrate possible scenarios for the enhancement of the Seebeck coefficient via the replacement of Ge in GeTe by [Ag+Sb] and show that tuning the carrier effective mass by changing the composition can be even more effective than tuning the carrier concentration.

In summary, the combination of the Seebeck coefficient and ^{125}Te NMR spin-lattice relaxation time measurements for $Ag_xSb_xGe_{50-2x}Te_{50}$ (well-known high-efficiency TAGS materials) provides a unique opportunity to elucidate the effects from both the carrier effective mass and concentration due to replacement of Ge in GeTe by [Ag+Sb]. The enhancement of the Seebeck effect, i.e. heat to electrical energy conversion, in these materials is primarily attributed to an increase of the carrier effective mass due to the interaction of mobile charge carriers with [Ag+Sb] atomic pairs.

The author thanks Materials Preparation Center at the Ames Laboratory, U.S. Department of Energy for samples synthesis, W. E. Straszheim, A. Howard, and Z. Swanson for help in experiments. This work was supported by the U. S. Department of Energy (DOE), Office of Science, Basic Energy Sciences, Materials Science and Engineering Division. The research was performed at the Ames Laboratory, which is operated for the U. S. Department of Energy by Iowa State University under Contract No DE-AC02-07CH11358.

E-mail: levin@iastate.edu

[1] G. J. Snyder and E.S. Toberer, Nat. Mater. **7**, 105 (2008).

[2] C. J. Vineis, A. Shakouri, A. Majumdar, and M. G. Kanatzidis, Adv. Mater. **22**, 3970 (2010).

[3] A. Shakouri, Annu. Rev. Mater. Res. **41**, 399 (2011).

[4] E. M. Levin, B. A. Cook, K. Ahn, M. G. Kanatzidis, and K. Schmidt-Rohr, Phys. Rev. B **80,** 115211 (2009).

[5] E. M. Levin, J. P. Heremans, M. G. Kanatzidis, and K. Schmidt-Rohr, Phys. Rev. B **88**, 115211 (2013).

[6] D. Koumoulis, T. C. Chasapis, R. E. Taylor, M. P. Lake, D., King, N. NB. Jarenwattananon,

G. A. Fiete, M. G. Kanatzidis, and L.-S. Bouchard, L.-S. Phys. Rev. Lett. **110**, 026602 (2013).

[7] D. Koumoulis, R. E. Taylor, D. King, Jr., and L.-S. Bouchard, Phys. Rev. B **90**, 125201 (2014).

[8] E. M. Levin, M. F. Besser, and R. Hanus, J. Appl. Phys. **114**, 083713 (2013).

[9] E. M. Levin, S. L. Bud'ko, and K. Schmidt-Rohr, Adv. Funct. Mater. **22**, 2766 (2012).

[10] H. Selbach, O. Kanert, and D. Wolf, Phys. Rev. B **19**, 4435 (1979).

[11] E. A. Skrabek and D. S. Trimmer, D. S. Properties of the general TAGS system. In *CRC Handbook of Thermoelectrics* (Ed. by D.M. Rowe) CRC Press LLC, 1995, chapter **22**.

[12] S. H. Yang, T. J. Zhu, T. Sun, J. He, S. N. Zhang, and S. B. Zhao, Nanotechnology **19**, 245707 (2008).

[13] J. R. Salvador, J. Yang, X. Shi, H. Wang, H., and A. A. Wereszczak, J. Solid State Chem. **182**, 2088 (2009).

[14] E. M. Levin, R. Hanus, M. Hamson, W. E. Strazheim, and K. Shmidt-Rohr. Phys. Status Solidi A **210**, 2628 (2013).

[15] J. P. Yesinowski, Top Curr. Chem. **306**, 229 (2012).

[16] Y. Gelbstein, B. Daro, O. Ben-Yehuda, Y. Sadia, Z. Dashevsky, and M. P. J. Dariel, Electron. Mater. **39**, 2049 (2010).

[17] M. S. Lubell and R. Mazelsky, J. Electrochem. Soc. **110**, 520 (1963).

[18] E. M. Levin. Phys. Rev. B **93**, 045209 (2016).

[19] N. V. Kolomoets, E. Ya. Lev, and L. M. Sysoeva, Sov. Phys.-Solid State **5**, 2871 (1964).

[20] Y. Chen, C. M. Jaworski, Y. B. Gao, H. Wang, T. J. Zhu, G. J. Snyder, J. P. Heremans, and X. B. Zhao, New J. Phys. **16**, 013057 (2014).

Table 1. Composition, acronym, [Ag+Sb] content, the Seebeck coefficient, S, ^{125}Te NMR spin-lattice relaxation time, T_1, the m^*_{TAGS} / m^*_{GeTe} and m^* / m_0 ratios for $Ag_xSb_xGe_{50-2x}Te_{50}$ (TAGS) materials at 300 K; the m^* / m_0 ratio was estimated based on our data for TAGS and using $m^* = 1.15\ m_0$ for GeTe [19].

Composition	Acronym	~[Ag+Sb] content (at.%)	S ($\mu V\ K^{-1}$) ±3 %	T_1 (ms) ±0.2 ms	$\frac{m^*_{TAGS}}{m^*_{GeTe}}$	m^*/m_0
GeTe	-	0	+34	5.3	-	1.15
$Ag_{1.5}Sb_{1.5}Ge_{47}Te_{50}$	TAGS-97	3.0	+38	4.2	1.14	1.31
$Ag_{2.8}Sb_{2.8}Ge_{44.4}Te_{50}$	TAGS-94	5.6	+48	3.8	1.33	1.53
$Ag_{4.5}Sb_{4.5}Ge_{41}Te_{50}$	TAGS-90	9.0	+60	3.6	1.51	1.74
$Ag_{6.5}Sb_{6.5}Ge_{37}Te_{50}$	TAGS-85	13.0	+83	3.1	1.83	2.12

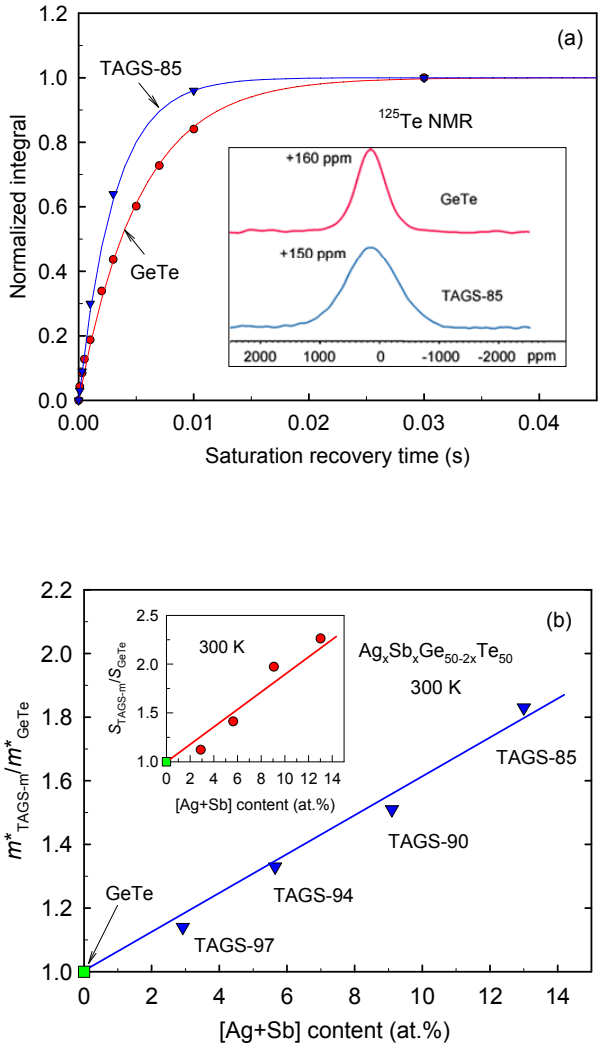

FIG. 1 (color online). (a) Dependence of normalized integral of ^{125}Te NMR signal vs. saturation recovery time measured at 300 K for the end compositions, GeTe and TAGS-85; inset in (a) shows ^{125}Te NMR spectra for the same materials. (b) The ratio of the effective masses in $Ag_xSb_xGe_{50-2x}Te_{50}$ (TAGS) and GeTe vs. [Ag+Sb] content at 300 K; inset in (b) shows the ratio of the Seebeck coefficients of the same materials vs. [Ag+Sb] content.

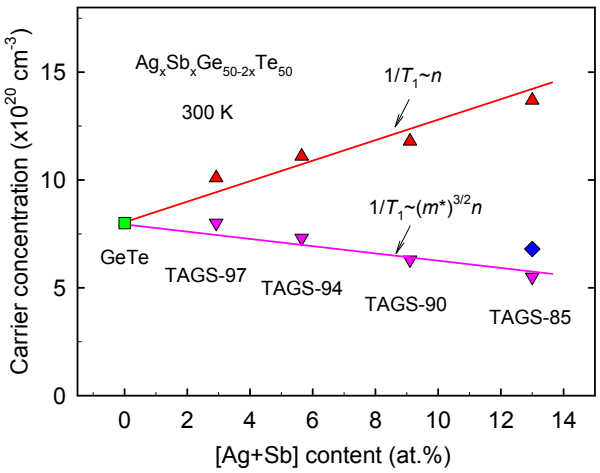

FIG. 2 (color online). Carrier concentration in $Ag_xSb_xGe_{50-2x}Te_{50}$ vs. [Ag+Sb] content at 300 K calculated from the values of ^{125}Te NMR spin-lattice relaxation times without (triangles) and with (inverted triangles) the effect from the carrier effective mass. Both the $1/T_1 \sim n$ and $1/T_1 \sim (m^*)^{3/2} n$ relations are based on classical Maxwell-Boltzmann statistics. The value of the carrier concentration in TAGS-85 (blue diamond) is obtained using the $1/T_1 \sim (m^*)^2 n^{2/3}$ relation, which is based on quantum Fermi-Dirac statistics.

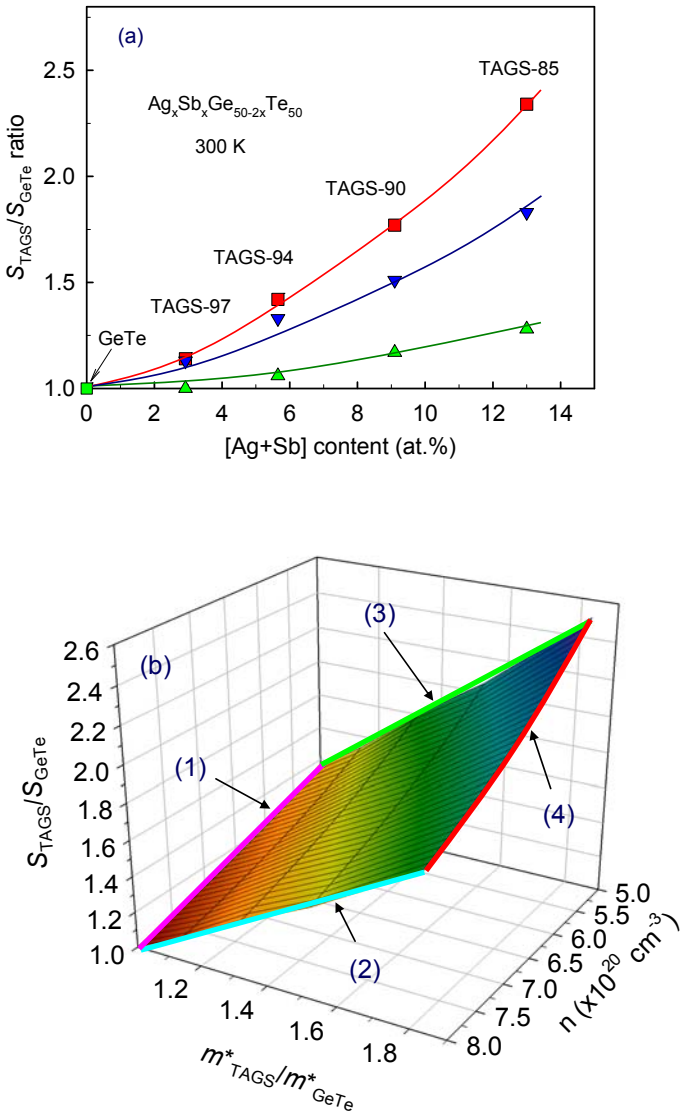

FIG. 3 (color online). (a) A total enhancement of the Seebeck coefficient in $Ag_xSb_xGe_{50-2x}Te_{50}$ at 300 K vs. [Ag+Sb] content (red squares) and the calculated contributions from a decrease of the carrier concentration (green triangles), and from an increase of the carrier effective mass (inverted blue triangles), and (b) the S_{TAGS}/S_{GeTe} ratio vs. the m^*_{TAGS}/m^*_{GeTe} ratio and carrier concentration, n; lines (1)-(4) show S_{TAGS}/S_{GeTe} vs. the: (1) carrier concentration when $m^*_{TAGS}/m^*_{GeTe}=1$, (2) carrier effective mass when $n = 8.0\times10^{20}$ cm^{-3}, (3) carrier effective mass when $n = 5.5\times10^{20}$ cm^{-3}, and (4) carrier concentration when $m^*_{TAGS}/m^*_{GeTe}=1.83$.